Supplementary data

Supplementary Appendix 1. Methods

The definitions of AMI, STEMI, NSTEMI, non-AMI and non-STEMI *[2-4]*

The definitions of AMI, STEMI, NSTEMI, non-AMI, and non-STEMI in this study are summarised in detail in **Supplementary Table 1**.

Data collection

ECG recordings were collected using a Philips 12-lead ECG machine (PH080A). The ECG signal was recorded in a digital format. The sampling frequency was 500 Hz, with 10 seconds recorded in each lead. Patient characteristics and laboratory tests were collected from our electronic medical records. The laboratory data collected closest to the time of the ECG were assigned to each ECG record. Because the ECG records were sometimes conducted within a relatively short time period, some ECGs from the same patients shared the same patient characteristics and laboratory data.

Timelines of door-to-balloon/CAG, door-to-ECG, and ECG-to-balloon/CAG

In STEMI patients without cardiac arrest, endotracheal intubation, or mechanical support, the mean door-to-balloon time was 65.7 min, the mean door-to-ECG time was 3.9 min, and the mean ECG-to-balloon time was 60.8 min. In STEMI patients with cardiac arrest, endotracheal tube intubation, or mechanical support, the mean door-to-balloon time was 205.6 min, the mean door-to-ECG time was 25.9 min, and the mean ECG-to-balloon time was 178.7 min. In NSTEMI patients, the mean door-to-CAG time was 629.6 min, the mean door-to-ECG time was 6.7 min, and the mean ECG-to-CAG time was 622 min.

Implementation of the deep learning model (DLM)

We developed a DLM with 82 convolutional layers and an attention mechanism. The technology details, such as the model architecture, data augmentation, and model visualisation, have been described previously [14]. We used the same architecture to train two new DLMs for AMI detection and infarct-related artery (IRA) analysis

of STEMI. The first DLM was trained via full samples with three categories, including STEMI, NSTEMI, and non-AMI, and the output of this model was a class-3 softmax output. The second DLM was trained via STEMI ECGs, and the output of this model was a class-4 softmax output for IRA analysis.

The standard input format of the DLM was a length of 1,024 numeric sequences, but the original length of our 12-lead ECG signals was 5,000. In the training process, we randomly cropped a length of 1,024 sequences as input. For the inference stage, nine overlapping lengths of 1,024 sequences based on interval sampling were used to generate a prediction and were averaged as the final prediction. Due to the scarcity of AMI cases in our study, an oversampling process was implemented to ensure that rare samples were adequately recognised. The settings for the training model were as follows: (1) Adam optimiser with standard parameters ($\beta_1 = 0.9$ and $\beta_2 = 0.999$) and a batch size of 36 for optimisation; (2) a learning rate of 0.001; and (3) a weight decay of 10^{-4}. The 100th epoch model was used as the final model, and the presented performance in the validation set was only evaluated once.

Implementation details of the DLM

The DLM architecture

The architecture of our DLM was based on ECG12Net, which was previously used for serum K+ concentration estimation [14]. Supposing that a standard 12-lead ECG signal comprised 12 sequences of N numbers (N = 1,250 in our database), the ECG signal sequence X = [x1,1, x1,2, …, x1,N; x2,1, x2,2, …, x2,N; …; x12,1, x12,2, …, x12,N] was used as the input, and the output was a one-hot encoder of AMI categories (STEMI, NSTEMI, and non-AMI) and the IRA of STEMI (STEMI-LMCA, STEMI-LAD, STEMI-LCx, and STEMI-RCA).

For example, a label of STEMI is encoded as [1,0,0], and a label of NSTEMI is encoded as [0,1,0]. Each output label corresponded to a segment of the input. Because the ECG information was mostly provided by morphologic changes with shift invariance, convolutional layers with weight sharing were used to adapt to this

situation and reduce the hazard of overfitting. We therefore developed a 12-channel sequence-to-sequence model to conduct this task as a revision of DenseNet. The complete architecture of the DLM is shown in **Supplementary Figure 1**. We defined a "dense unit" as a neural combination as follows: (1) a batch normalisation layer to normalise input data, (2) a rectified linear unit (ReLU) layer for non-linearisation, (3) a 1×1 convolution layer with 4K filters to reduce the dimensions of the data, (4) a batch normalisation layer for normalisation, (5) a ReLU layer for non-linearisation, (6) a 3×1 convolution layer with 4K filters to extract features, (7) a batch normalisation layer for normalisation, (8) a ReLU layer for non-linearisation, and (9) a 1×1 convolution layer with K filters to extract features. K was a model constant that was set at 32 in all our experiments. After using a dense unit to extract features, we used the dense connectivity resulting from direct connections from any layer to all subsequent layers to build a "dense block". We designed a model with five dense blocks comprising 3,3,6,6, and three dense units.

Dense blocks cannot be concatenated when the size of the feature maps changes. Thus, a pooling block was used to concatenate each dense block for downsampling in our architecture. This block included a dense unit with a 2×1 stride and an average pooling layer with a 2×1 kernel size and stride, which was used for downsampling. Each dense block was concatenated by the pooling block to integrate the features of the previous blocks.

A length of 864 numeral sequences was used as the input in our experiment. We designed an ECG lead block with 80 trainable layers, the architecture of which is shown in **Supplementary Figure 1A**. The input data were passed through a batch normalisation layer, followed by a convolution layer, another batch normalisation layer, a ReLU layer, and a pooling layer. The initial convolution layer comprised *K* convolution filters with a kernel size of 7×1 and a stride of 2×1. Next, the data were passed through a series of dense blocks and a pooling block, resulting in a 16×1×864 array. A ReLU layer, a batch normalisation layer, and a global pooling layer were followed by the last dense block. Finally, a fully connected layer with *k* output was created for follow-up use, where *k* is the number of categories, which was equal to 3 in the first AMI detection model and 4 in the second

IRA analysis model of STEMI. This ECG lead block was used to extract 864 features from each ECG lead, making a basic output prediction based on each lead. **Supplementary Figure 1B** shows how ECG12Net integrated all the information from the ECG to make an overall prediction. ECG12Net comprised 12 ECG lead blocks corresponding to lead sequences. We designed an attention mechanism based on a hierarchical attention network to concatenate these blocks, increasing the interpretive power of ECG12Net. The attention block comprised a batch normalisation layer followed by a fully connected layer and then two combinations of a batch normalisation layer, a ReLU layer, and a fully connected layer. The first and second fully connected layers each contained 8/*k* neurons. Attention scores were calculated for each ECG lead and then integrated for standardisation by a linear output layer. The standardised attention scores were used to weight the 12 ECG lead outputs by simple multiplication. The 12 weighted outputs were summed and converted into a softmax output layer to provide the final prediction value. The above model using ECG information was named ECG12Net, which contained 82 trainable layers. The m-log-loss function was used to calculate model loss. A dropout layer was added only in the fully connected layer, and the dropout rate was set to 0.5.

Training details

The 12-lead ECG signal sequences were first trained by the 12 ECG leads separately. Due to the seriously uneven distribution in STEMI, NSTEMI, and non-AMI, an oversampling process was implemented to improve performance by ensuring that rare samples were adequately recognised. We sampled 12 STEMI ECGs, 12 NSTEMI ECGs, and 12 non-AMI ECGs in each batch. This process sufficiently considered rare STEMI and NSTEMI cases so as not to be skewed by the overwhelming number of normal cases. We used the software package MXNet version 1.3.0 to implement ECG12Net. The settings used for the training model were as follows: (1) Adam optimiser with standard parameters (β_1 = 0:9 and β_2 = 0:999) and a batch size of 36 for optimisation; (2) initial learning rate set at 0.001 and lowered by 10 three times when validation loss plateaued after an epoch; and (3) a weight decay of 10^{-4}. Because the sampling rate of our machine is 500 Hz, our 12-lead ECG signal includes 12 numeral sequences with 5,000 digits. However, the standard input format of ECG12Net was a length of 1,024 numeric sequences. We randomly cropped a length of 1,024 sequences as input in the

training process. During the inference stage, the nine overlapping lengths of 1,024 sequences based on interval sampling (X_1 to X_{1024}, X_{498} to X_{1521}, X_{995} to X_{2018}, X_{1492} to X_{2515}, X_{1989} to X_{3012}, X_{2486} to X_{3509}, X_{2983} to X_{4006}, X_{3480} to X_{4503}, and X_{3977} to X_{5000}) were used to generate predictions and averaged as the final prediction. The 100^{th} epoch model was used as the final model, and the model performance in the validation set was verified only once.

Data augmentation

A previous study reported severe overfitting in an atrial fibrillation detection task and suggested a series of data augmentations to improve model performance. In the current study, the problem of overfitting was due to the large number of parameters in the deep learning architecture (~3 million trainable parameters) relative to the sample size. The first step in tackling this issue was to resize the sequence length by adjusting heart rate. We randomly resampled a broader range of heart rates in a uniform distribution from 0.8 *HR* to 1.2 *HR*, where *HR* was the original heart rate for each sample. The second step was to randomly crop a length of 1,024 sequences as input. The third step was to add a random variable drawn from a Gaussian distribution with a mean of 0 and a standard deviation of 0.1. Fourth, time points were selected uniformly and at random, and the ECG signal values within a 50 ms vicinity of these points were set at 0. This method was called dropout burst. Finally, we set six random ECG lead sequences to 0 in the combined training step. We observed that the final DLM only used information from a few ECG leads to make a prediction and inferred that the model had ceased to learn features from the other ECG leads because it had perfectly predicted all the data in the training set. This approach forced the DLM to learn all the abnormal ECG leads.

Model visualisation

To interpret the network predictions, we conducted heatmaps to visualise the ECG rhythms and leads using class activation mappings (CAMs) and attention mechanisms based on the global average pooling (GAP) architecture in the last network, which was used at the end of each ECG lead. In addition, the various

contributions each ECG lead made to the final prediction were weighted by the attention mechanisms, which were used to visualise the importance of each ECG lead.

Summary of the research interests, model comparison and statistical methods

The research interests, model comparison and statistical methods in this study are summarised in detail in **Supplementary Table 2**.

Supplementary Appendix 2. Results

The baseline characteristics of the cohorts

The characteristics and laboratory data are shown in **Supplementary Table 3**. Patients in the validation cohort were significantly older, had more comorbidities, had impaired estimated glomerular filtration rates and alanine aminotransferase, lower cTnI, and higher glucose and low-density lipoprotein cholesterol levels than those in the development cohort. The development/validation cohorts consisted of 860/191, 559/138, and 109,904/30,432 STEMI, NSTEMI, and non-AMI ECGs, respectively. The LAD and RCA were the most commonly identified IRAs in STEMI. Patients with STEMI were more likely to be male, to be overweight, to have prior coronary artery disease (CAD), and to have higher cTnI and more impaired lipid profiles than those in the non-AMI group. Patients with NSTEMI were more likely to be male, be older and have prior CAD and more comorbidities, higher cardiac biomarkers, and more impaired lipid profiles than those in the non-AMI group.

ECG lead-specific analysis

The ECG lead-specific analyses for the detection of STEMI and the corresponding IRA are shown in **Supplementary Figure 4**. ECG leads were specifically analysed for the detection of STEMI in the hypothetical real world. Leads III, V2, aVL, and V3 demonstrated better performance than the other leads for the detection of STEMI, with the AUCs of 0.913, 0.913, 0.911, and 0.908, respectively. For the detection of the IRA of STEMI, lead-specific ROC curve analysis on the IRA of STEMI demonstrated that the best performances for

the LAD were V4, V2, and V3 with AUCs of 0.970, 0.955, and 0.953, respectively, and those for the RCA were aVL, lead III, and aVF with AUCs of 0.995, 0.978, and 0.966, respectively.

Discussion

With the aid of the first recorded cTnI, the DLM exhibited an excellent diagnostic yield with an AUC of 0.978 for NSTEMI detection, which was significantly better than those of the DLM or cTnI alone, with AUCs of 0.877 and 0.949, respectively. The universal diagnosis of NSTEMI is derived from the clinical presentation, 12-lead ECG, and cardiac troponin levels. To date, biomarker measurement for myocardial injury, preferably high-sensitivity cardiac troponin, was mandatory in all patients with suspected NSTEMI due to its high sensitivity and specificity [4]. However, several concerns should be considered in current practice. First, the guidelines suggest that the second cardiac troponin assessment be performed 1-3 hours after the first blood test in unconfirmed cases. Repeated time-consuming laboratory tests might delay the diagnosis. Second, cardiac troponin levels might be perturbed in some clinical conditions other than AMI. Combined with the information of the first recorded cTnI, the DLM allows rapid and powerful NSTEMI detection in patients at high or very high risk.

Regarding NSTEMI detection, DLM showed less sensitivity than the cardiologists. Several points should be clarified. Among the 58 NSTEMI ECGs unrecognised by the DLM, there were several atypical ECG presentations, including intraventricular conduction disorders, ventricular hypertrophy, poor R wave progression, or baseline variants. Even experienced cardiologists could not identify some of these ECGs. Moreover, overdiagnosis of NSTEMI by ECG is commonplace in clinical practice, which may partially explain the high sensitivity and low specificity of the performance of the physicians in this study. With the aid of the DLM with its high specificity in the detection of NSTEMI, physicians could exclude NSTEMI early, which reduced subsequent lab tests, ED observation time and guided physicians to differentiate it from other diagnoses unrelated to AMI. As a result, it was worthwhile to increase the ECG training data along with the first-record cTnI to enhance the capacity of the DLM in NSTEMI detection in the future.

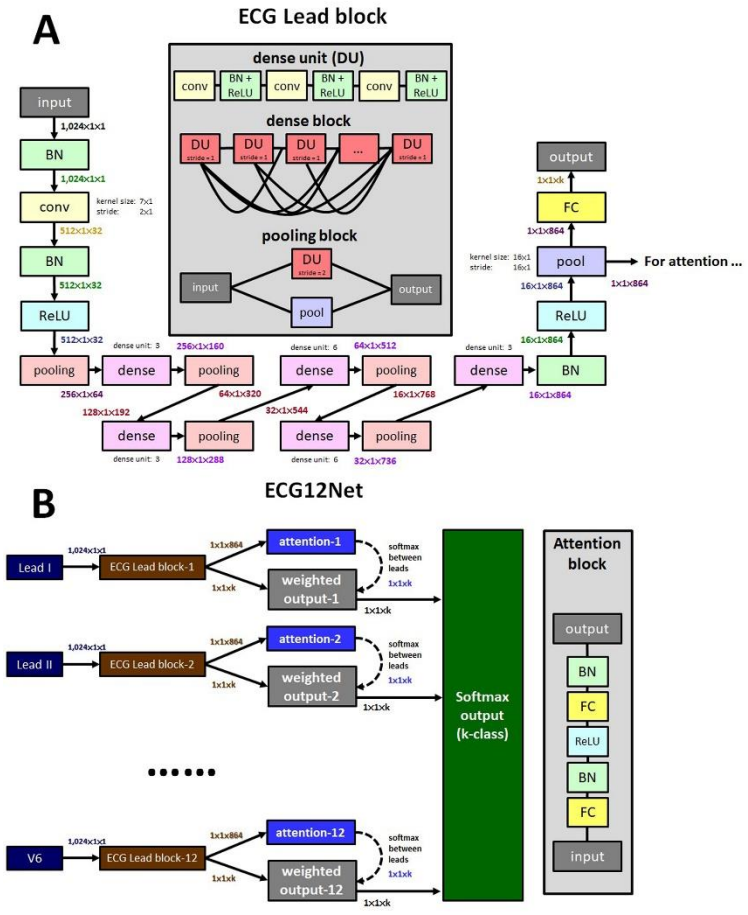

Supplementary Figure 1. Architecture of the DLM.

A) Electrocardiography (ECG) lead block with 80 trainable layers.

B) The DLM integrated all the information from the ECG leads to make an overall prediction. The bold and coloured words denote the output dimensions of the layers and the black words signify the important role for the layers. The model constant K was equal to 32 for all the dense blocks and pooling blocks.

BN: batch normalisation; Conv: convolution; FC: fully connected; ReLU: rectified linear unit

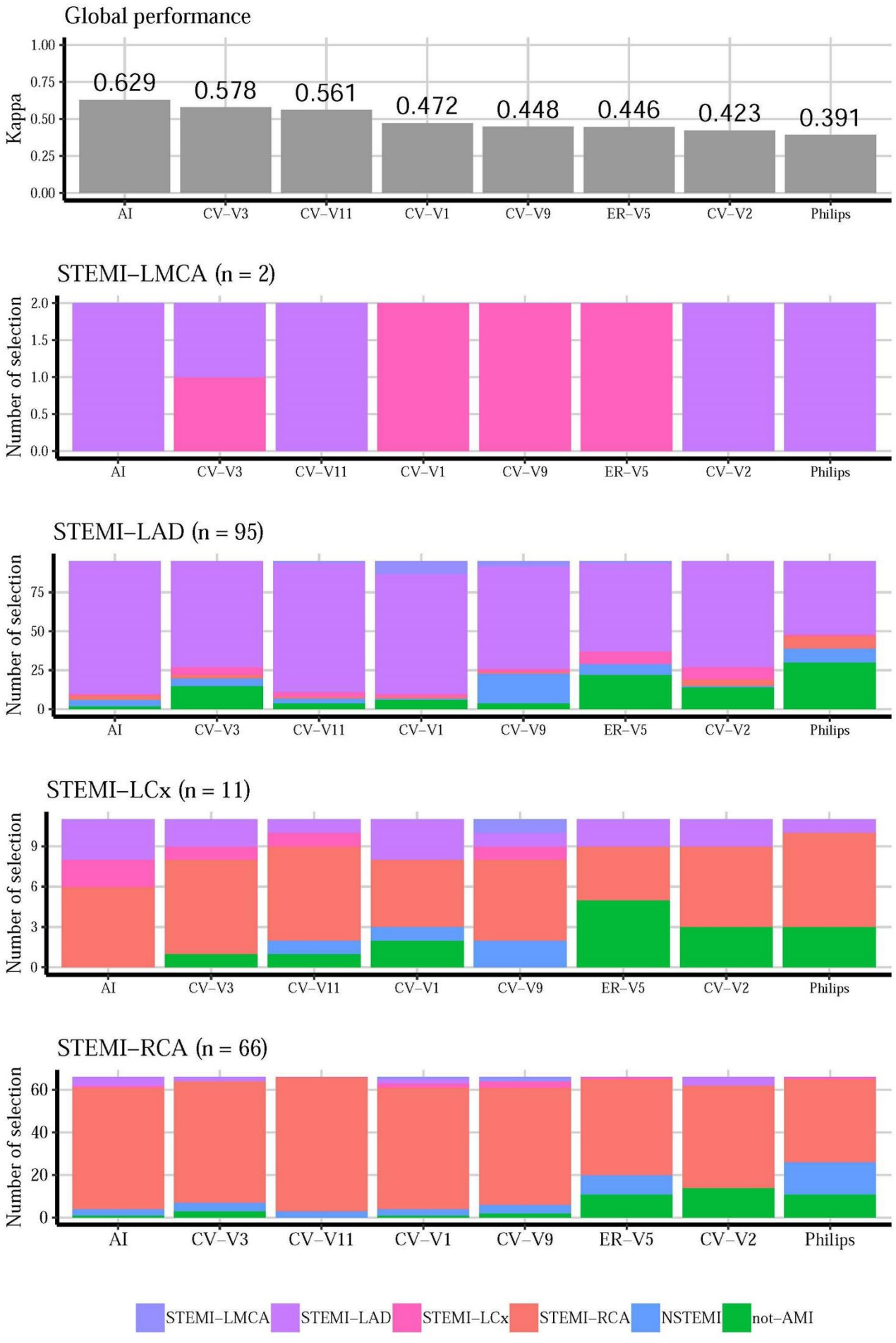
Global performance
Kappa
1.00
0.75
0.50
0.25
0.00
0.629
0.578
0.561
0.472
0.448
0.446
0.423
0.391
AI
CV–V3
CV–V11
CV–V1
CV–V9
ER–V5
CV–V2
Philips
STEMI–LMCA (n = 2)
Number of selection
2.0
1.5
1.0
0.5
0.0
STEMI–LAD (n = 95)
75
50
25
0
STEMI–LCx (n = 11)
9
6
3
0
STEMI–RCA (n = 66)
60
40
20
0
STEMI–LMCA
STEMI–LAD
STEMI–LCx
STEMI–RCA
NSTEMI
not–AMI

Supplementary Figure 2. Performance rankings of infarct-related artery detection of STEMI among DLM, physicians and the Philips algorithm in the human-machine competition.

Global performance rankings based on the 6-class kappa values. V(X) denoted the (V) visiting staff with (X) years of experience. The infarct-related arteries of STEMI were classified into the LMCA, LAD, RCA and LCx.

LAD: left anterior descending artery; LCx: left circumflex artery; LMCA: left main coronary artery; RCA: right coronary artery

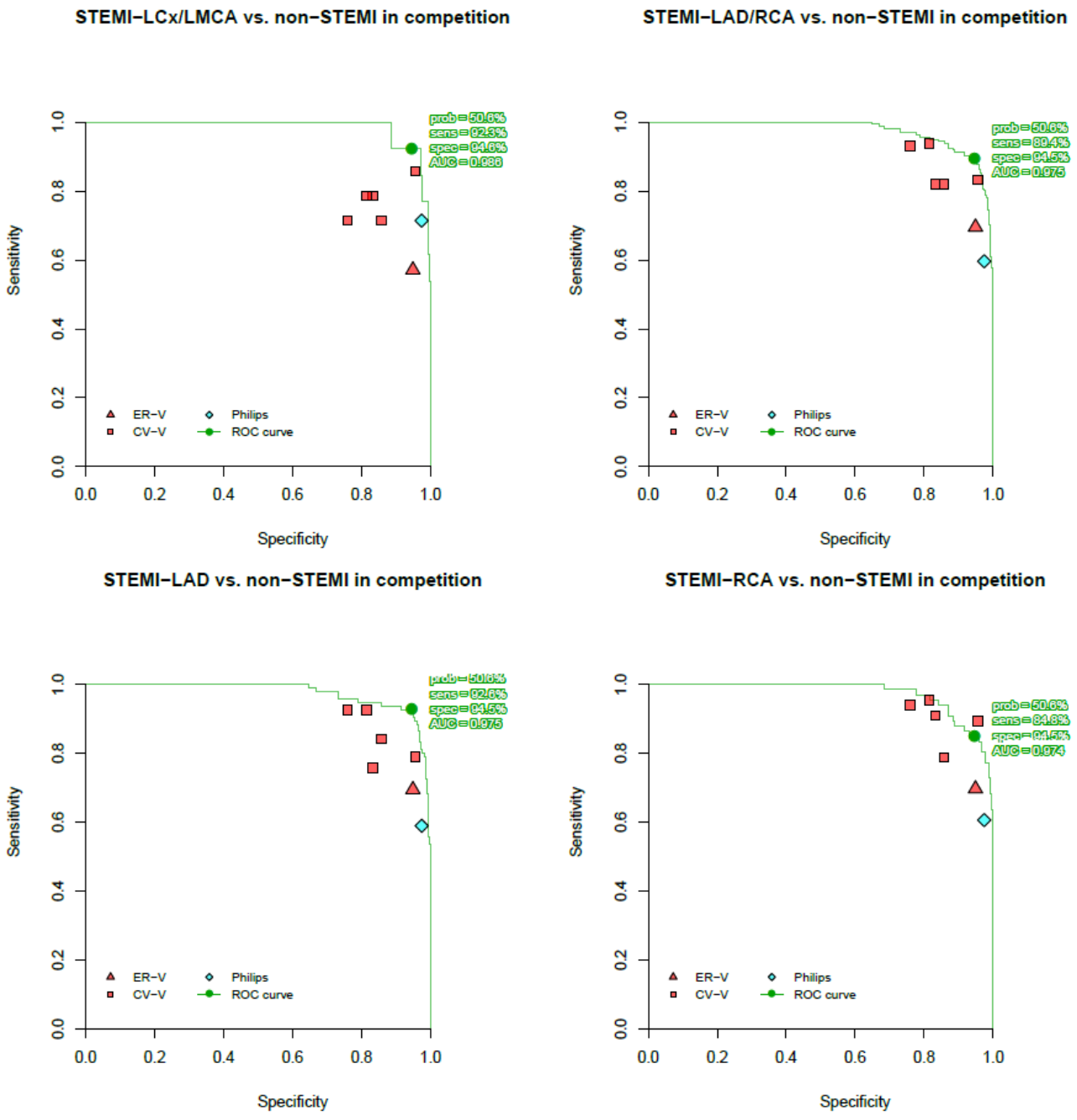

Supplementary Figure 3. Performance comparison for anterior (LAD), inferior (RCA), and combined anterior and inferior (LAD+RCA) STEMI detection in the human-machine competition.

The area under the receiver operating characteristic curve (AUC) was generated by the prediction of the DLM. The triangles, the square and the diamond denote the cardiologists, the emergency physician and the Philips algorithm, respectively.

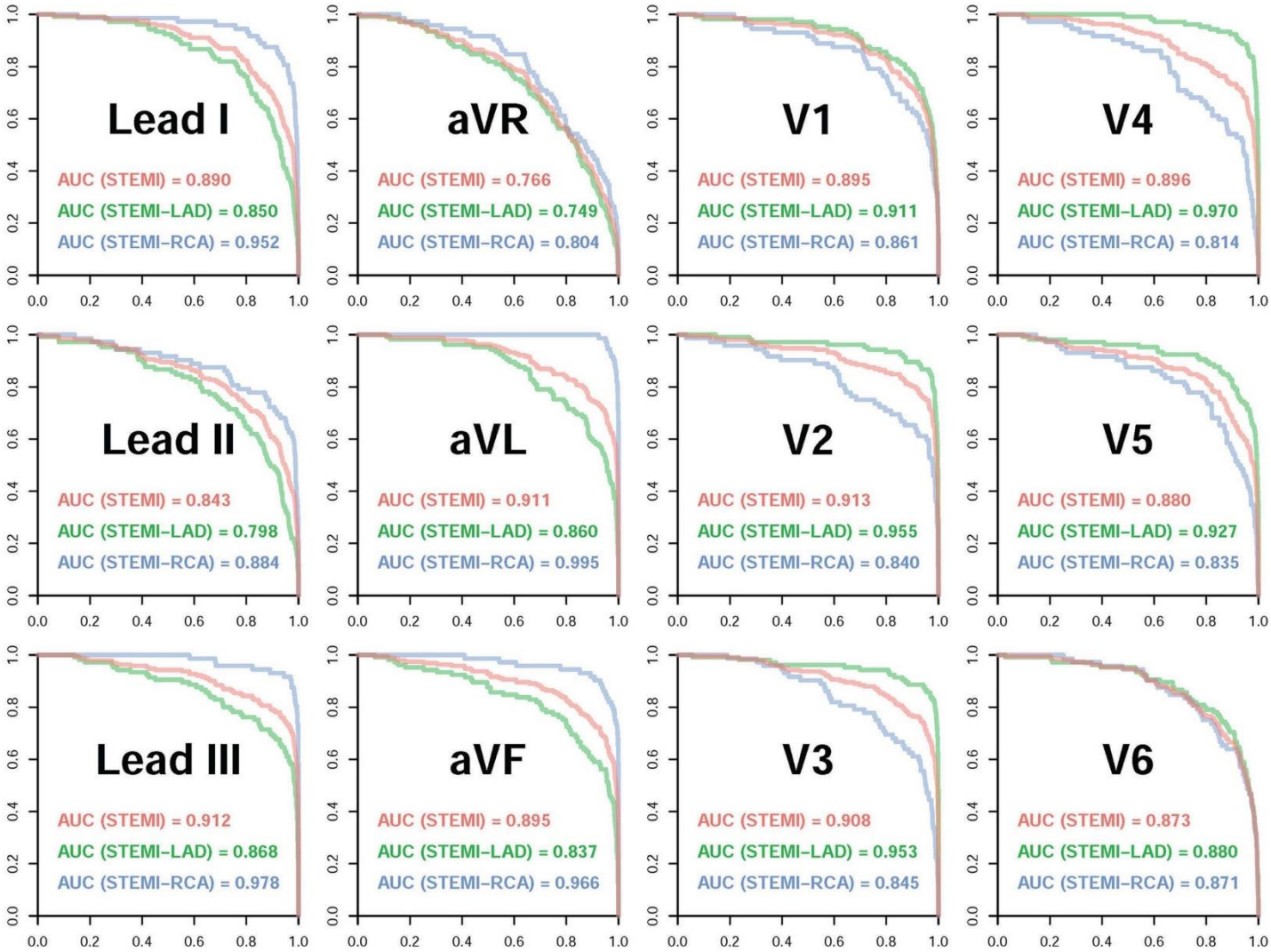

Supplementary Figure 4. ECG lead-specific analyses for the detection of STEMI, STEMI-LAD and STEMI-RCA.

The receiver operating characteristic (ROC) curves with the specificity on the x-axis and the sensitivity on the y-axis were generated by the DLM for the detection of STEMI and the corresponding IRA in the revised proportion of the hypothetical real world (STEMI = 0.1%, NSTEMI = 0.2%, and non-AMI = 99.7%). The controls were the non-AMI samples.

AUC: area under the ROC curve

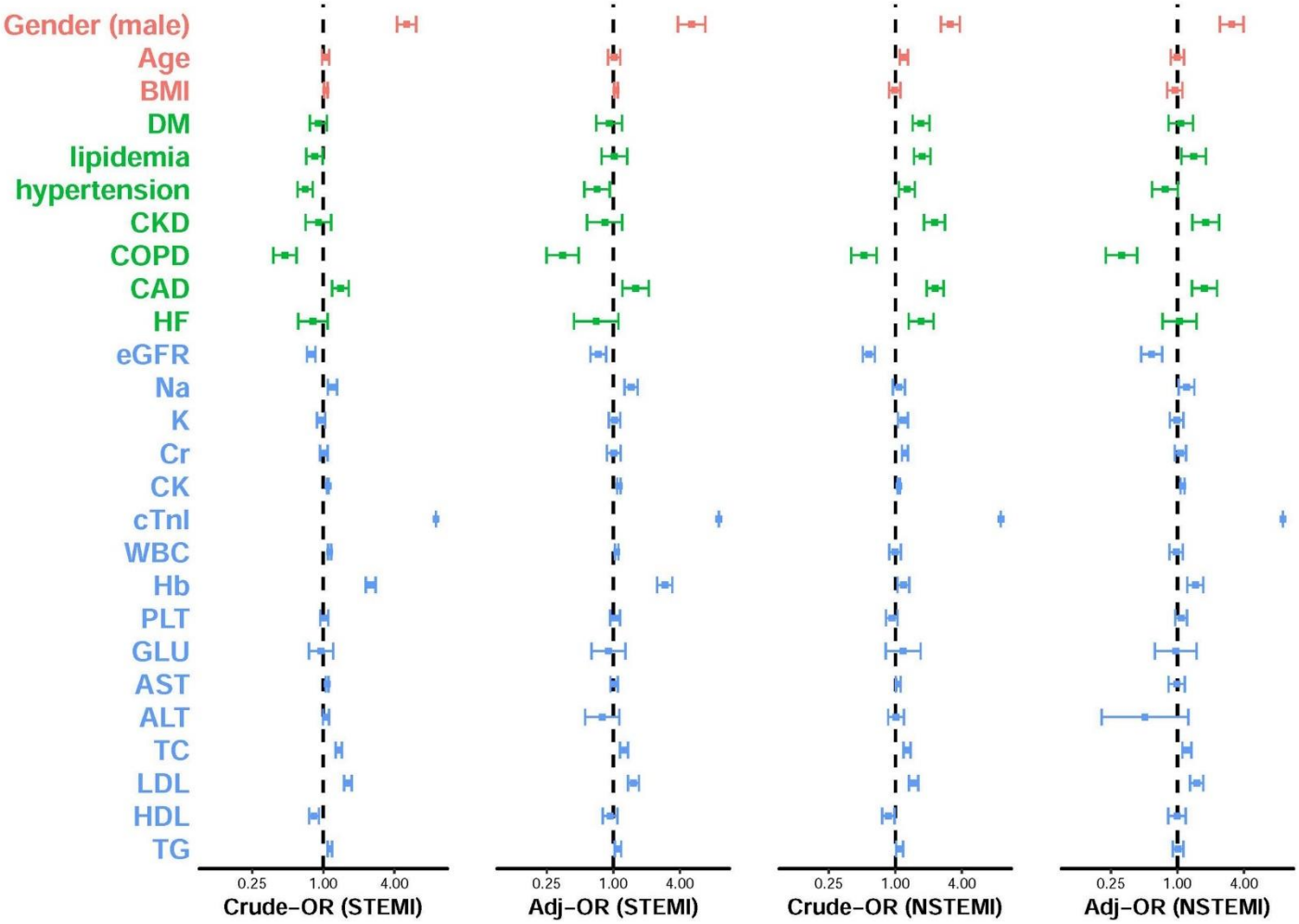

Supplementary Figure 5. Univariate and multivariate logistic regression analysis of STEMI, and NSTEMI in the development cohort.

The controls in all analyses were non-AMI samples. The adjusted variables included gender, age, body mass index, and all disease histories. The continuous variables were standardised by the mean and standard deviation. The units of each continuous variable were one standard deviation.

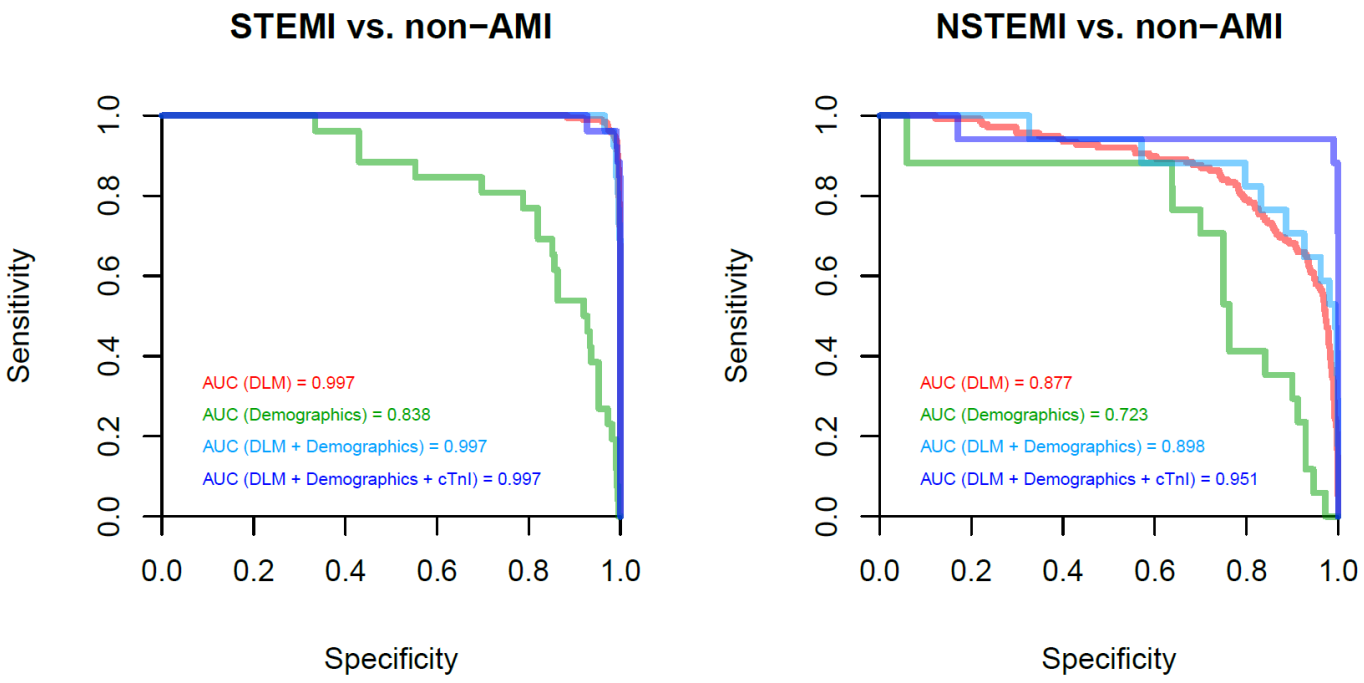

Supplementary Figure 6. Comparison of the diagnostic value among additional demographic variables, cTnI and DLM in the validation cohort.

The receiver operating characteristic (ROC) curves were generated from the logistic regression analysis using the development cohort. Patient demographic variables to predict (5A) STEMI and (5B) NSTEMI included gender, age, BMI, CAD, eGFR, and Hb. (5A) DLM vs DLM + Demographics vs DLM + Demographics + cTnI, p=ns; DLM or DLM + Demographics or DLM + Demographics + cTnI vs Demographics, p<0.0001. (5B) DLM vs Demographics, p<0.05; DLM + Demographics + cTnI vs DLM + Demographics, p=0.08.

AUC: area under the ROC curve

A. de Winter sign

B. Wellens' syndrome, type I

C. Wellens' syndrome, type II

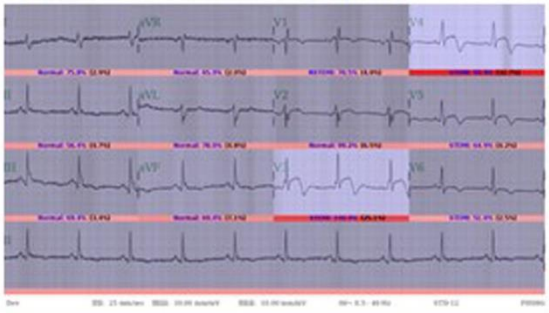

D. Posterior wall MI

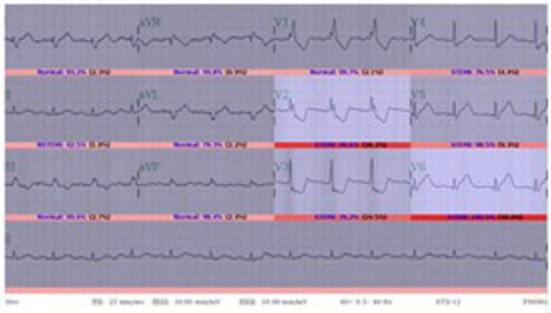

E. aVR ST elevation

F. Hyperacute T

G. LBBB

H. RBBB

Supplementary Figure 7. The test examples of the detection of STEMI equivalents by the DLM.

STEMI equivalents including de Winter sign, Wellens' syndrome, posterior wall MI, ST elevation in lead aVR with diffuse ST depression, hyperacute T-waves and ST elevation in the presence of bundle branch block. The prediction rate of STEMI in each example of STEMI equivalent ECG by the DLM is shown in each figure.

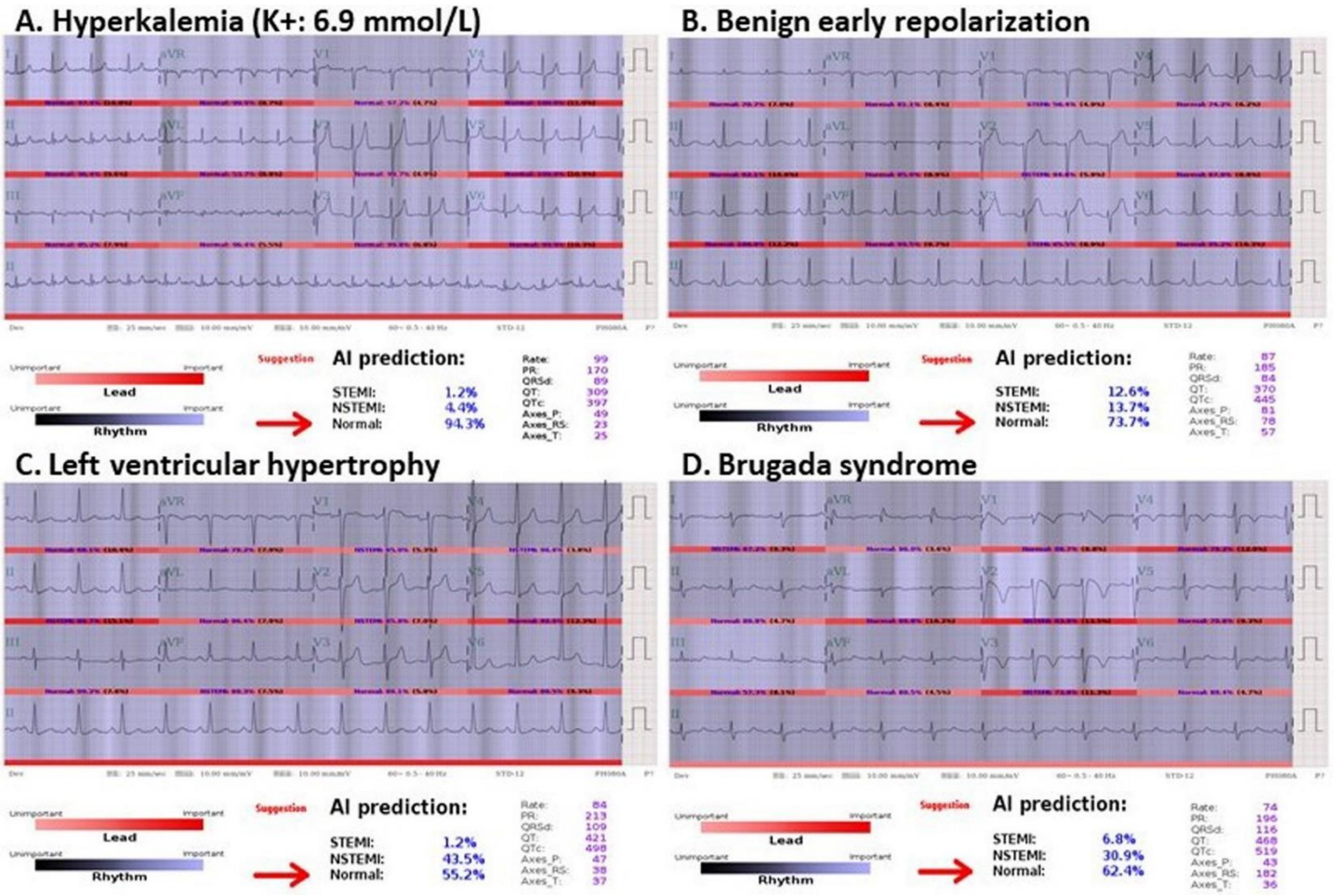

Supplementary Figure 8. The test examples of the detection of high take-off T ECG by the DLM. High take-off T ECG including hyperkalaemia, benign early repolarisation, left ventricular hypertrophy, and Brugada syndrome. The prediction rate of STEMI in each example of high take-off T ECG by the DLM is shown in each figure.

Supplementary Table 1. The definitions of AMI, STEMI, NSTEMI, non-AMI and non-STEMI.

Groups	Definition and inclusion in this study
AMI	AMI included symptoms of myocardial ischaemia, the ECG presentation and the elevated cTnI (above the 99th percentile of the upper reference limit of healthy individuals), which included both STEMI and NSTEMI
STEMI	AMI patients with ST-segment elevation on ECG who were validated by CAG
NSTEMI	AMI patients without ST-segment elevation on ECG who were validated by CAG
Non-AMI	Patients with a normal cTnI series during an ED stay who had neither STEMI nor NSTEMI
Non-STEMI	NSTEMI and non-AMI

AMI: acute myocardial infarction; CAG: coronary angiogram; cTnI: conventional cardiac troponin I; ECG: 12-lead electrocardiogram; ED: emergency department; NSTEMI: non-ST-segment elevation myocardial infarction; STEMI: ST-segment elevation myocardial infarction

Supplementary Table 2. The research interests, model comparison and statistical methods.

Figures	Purpose	Comparison	Methods
Figure 1	To compare the performance between the DLM and physicians in detecting STEMI by ECGs in the human-machine competition.	STEMI vs non-STEMI	AUC-ROC curve, PRROC curve with sensitivity (recall), specificity, and positive predictive value (precision).
Figure 2	To compare the performance of STEMI detection among the DLM, the physicians and the Philips algorithm.	DLM vs physicians, Philips algorithm	The performance (kappa value) and consistency analysis.
Figure 4A	To compare the performance of the DLM, cTnI and the DLM plus cTnI in detecting STEMI in the validation cohort	STEMI vs non-AMI	AUC-ROC curve.
Figure 4B	To compare the performance of the DLM, cTnI and the DLM plus cTnI in detecting NSTEMI in the validation cohort.	NSTEMI vs non-AMI	AUC-ROC curve.

AMI: acute myocardial infarction; AUC-ROC: area under the receiver operating characteristic curve; CAG: coronary angiogram; cTnI: cardiac troponin I; DLM: deep learning model; ECG: 12-lead electrocardiogram; NSTEMI: non-ST-segment elevation myocardial infarction; STEMI: ST-segment elevation myocardial infarction

Supplementary Table 3. Corresponding patient characteristics and laboratory results of STEMI, NSTEMI, and non-AMI ECGs in the development and validation cohorts.

	Development cohort				Validation cohort				*p*-value#
	STEMI (n=860)	**NSTEMI (n=559)**	**non-AMI (n=109,904)**	***p*-value**	**STEMI (n=191)**	**NSTEMI (n=138)**	**non-AMI (n=30,432)**	***p*-value**	
STEMI location									
STEMI-LMCA	21 (2.4%)				3 (1.6%)				
STEMI-LAD	420 (48.8%)				105 (55.0%)				
STEMI-LCx	87 (10.1%)				11 (5.8%)				
STEMI-RCA	332 (38.6%)				72 (37.7%)				
Gender (male)	688 (83.8%)	420 (76.2%)	55,453 (50.5%)	<0.001	150 (82.9%)	84 (62.2%)	15,484 (50.9%)	<0.001	0.369
Age (years)	61.8±13.8	64.3±13.8	60.9±19.6	<0.001	62.9±14.6	65.9±13.7	62.6±20.2	0.165	<0.001
BMI (kg/m^2)	25.9±4.5	24.4±3.9	24.5±8.8	0.009	26.9±4.7	25.0±4.9	24.5±6.0	0.043	0.575
Disease history									
CAD	197 (24.0%)	188 (34.1%)	20,275 (18.4%)	<0.001	133 (73.5%)	95 (70.4%)	7,439 (24.4%)	<0.001	<0.001
HF	50 (6.1%)	66 (12.0%)	8,099 (7.4%)	<0.001	21 (11.6%)	33 (24.4%)	2,972 (9.8%)	<0.001	<0.001
DM	176 (21.4%)	187 (33.9%)	25,429 (23.1%)	<0.001	39 (21.5%)	50 (37.0%)	7,675 (25.2%)	0.004	<0.001
HTN	249 (30.3%)	243 (44.1%)	42,081 (38.3%)	<0.001	67 (37.0%)	83 (61.5%)	14,177 (46.6%)	<0.001	<0.001
CKD	68 (8.3%)	101 (18.3%)	9,929 (9.0%)	<0.001	8 (4.4%)	26 (19.3%)	2,332 (7.7%)	<0.001	<0.001
Hyperlipidaemia	198 (24.1%)	219 (39.7%)	30,087 (27.4%)	<0.001	34 (18.8%)	53 (39.3%)	8,579 (28.2%)	<0.001	0.007
COPD	85 (10.4%)	62 (11.3%)	21,600 (19.7%)	<0.001	24 (13.3%)	19 (14.1%)	7,090 (23.3%)	<0.001	<0.001
Laboratory test									
Na (mEq/L)	137.3±3.2	136.9±3.6	136.6±4.5	<0.001	137.1±2.7	135.9±3.4	135.8±4.7	0.005	<0.001
K (mEq/L)	3.9±0.6	4.0±0.6	3.9±0.5	0.006	3.8±0.5	4.0±0.6	3.9±0.5	0.008	0.211
eGFR (mL/min)	74.2±26.3	63.8±30.7	82.5±37.0	<0.001	74.2±26.5	64.3±37.4	81.0±35.0	<0.001	<0.001
Cr (mg/dl)	1.3±1.3	1.9±2.2	1.3±1.6	<0.001	1.3±0.9	2.3±2.6	1.2±1.3	<0.001	<0.001
CK (ng/mL)	389.8±650.7	296.1±325.4	131.7±409.0	<0.001	348.9±597.0	252.5±310.7	122.5±306.9	<0.001	<0.001
cTnI (ng/mL)	60.6±598.7	224.8±1,121.7	0.0±0.0	<0.001	4.8±16.6	2.7±6.5	0.0±0.0	<0.001	0.015
WBC (10^3/ul)	11.1±3.6	8.8±3.0	8.9±4.5	<0.001	11.2±3.2	9.3±2.8	8.8±4.6	<0.001	0.125
Hb (gm/dl)	14.6±1.9	13.2±2.4	12.9±2.3	<0.001	14.7±1.7	13.2±2.7	12.9±2.3	<0.001	0.120
PLT (10^3/ul)	228.5±64.0	221.0±74.6	227.0±81.9	0.425	228.4±90.7	216.5±52.9	210.1±74.9	0.015	<0.001
GLU (gm/dl)	193.9±85.3	219.4±126.3	198.7±114.8	0.631	166.0±13.1	215.8±85.5	241.1±128.5	0.462	<0.001
AST (U/L)	54.0±85.3	45.6±104.5	32.6±81.3	<0.001	51.3±65.0	36.4±37.1	33.0±91.3	0.075	0.590
ALT (U/L)	41.3±73.4	34.2±78.9	32.8±93.1	0.215	44.6±21.3	39.0±40.6	79.0±200.9	0.762	<0.001
TC (gm/dl)	172.0±40.9	168.4±37.5	148.8±47.7	<0.001	173.6±36.8	162.8±38.3	147.6±48.0	<0.001	0.081
LDL (gm/dl)	111.4±33.7	106.8±33.8	89.7±36.3	<0.001	116.4±33.2	103.2±28.0	95.9±38.2	<0.001	<0.001
HDL (gm/dl)	38.7±9.0	39.2±9.4	41.2±14.4	<0.001	41.5±10.4	35.3±9.8	42.0±15.0	0.007	0.295
TG (gm/dl)	153.4±148.7	137.0±73.4	118.0±127.8	<0.001	120.3±55.8	157.7±96.2	116.6±160.7	0.043	0.354

The hypothesis test between the development cohort and the validation cohort.

ALT: alanine aminotransferase; AST: aspartate aminotransferase; BMI: body mass index; CAD: coronary artery disease; CK: creatine kinase; CKD: chronic kidney disease; COPD: chronic obstructive pulmonary disease; Cr: creatinine; cTnI: conventional cardiac troponin I; DM: diabetes mellitus; eGFR: estimated glomerular filtration rate; GLU: glucose; Hb: haemoglobin; HDL: high-density lipoprotein cholesterol; HF: heart failure; HTN: hypertension; K: potassium; LAD: left anterior descending artery; LCx: left

circumflex artery; LDL: low-density lipoprotein cholesterol; LMCA: left main coronary artery; Na: sodium; PLT: platelet; RCA: right coronary artery; TC: total cholesterol; TG: triglyceride; WBC: white blood cell count